Extended Two-Channel Kondo Phase of a Rotational Quantum Defect in a Fermi Gas

E Fuh Chuo[1], K Ballmann[1], L Borda[2] and J Kroha[1]

[1] Physikalisches Institut, Universität Bonn, Nussallee 12, 53115 Bonn, Germany
[2] Department of Theoretical Physics, Budapest University of Technology and Economics, Budafoki ut 8, H-1111 Budapest, Hungary

E-mail: kroha@physik.uni-bonn.de

Abstract. We show by exact numerical renormalization group calculations that a quantum defect with a two-dimensional rotational degree of freedom, immersed in a bath of fermionic particles with angular momentum scattering, exhibits an extended 2CK phase without fine-tuning of parameters. It is stabilized by a correlation effect which causes the states with angular momentum $m = \pm 1$ to be the lowest energy states of the defect. This level crossing with the non-interacting $m = 0$ ground state is signaled by a plateau in the temperature-dependent impurity entropy at $S(T) = k_B \ln 2$, before the 2CK ground state value $S(0) = k_B \ln \sqrt{2}$ is reached.

1. Introduction

The two-channel Kondo (2CK) effect has intrigued condensed matter physicists ever since the problem has been formulated by Noziéres and Blandin in 1980 [1]. It arises when two identical baths or "channels" of mobile fermionic particles compete for the formation of a singlet with a quantum impurity spin S=1/2. As a result, an exotic quantum state of matter with a non-vanishing zero-point entropy of $S(0) = k_B \ln \sqrt{2}$ is formed, and the very notion of particles comprising the system breaks down [2, 3, 4]. However, the necessity of fine-tuning of system parameters to the symmetry point where the quantum impurity degree of freedom is degenerate as well as the two channels are identical (i.e., they have the same density of states and the same coupling to the impurity), has hampered the physical realization of the 2CK effect in electronic systems, see Ref. [5] for a review. For two-level systems (TLS) in a metal, proposed early-on to exhibit the 2CK effect [6], it was shown that the Kondo temperature T_K is generically lower than the TLS level splitting concatenated with the TLS tunneling transitions, so that the 2CK fixed point could not be reached [7, 8]. The realization in heavy-fermion lattice systems, albeit supported by symmetries stabilizing the 2CK fixed point [5], has remained unconfirmed due to the multitude of unclear experimental signatures [9, 10]. In an ingeneously designed semiconductor quantum dot system 2CK signatures could only be observed by fine-tuning of system parameters [11, 12].

In the present work we consider a rotational quantum defect immersed in a fermionic bath. The defect can be comprised of an atomic particle bound in a flattened or effectively two-dimensional harmonic oscillator potential. The three lowest quantum states of the isolated defect are the ground state with angular momentum $m = 0$ and a doublet of degenerate angular

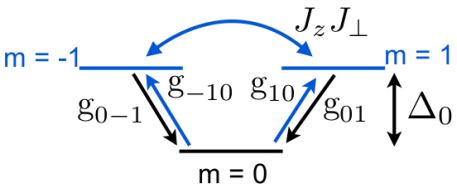

Figure 1. Level scheme of the SU(3) impurity showing the different coupling constants of the local level transitions and the level splitting Δ_0.

momentum states $m = \pm 1$, split off from the ground state by an excitation energy Δ_0, see Fig. 1. Upon coupling to the itinerant fermion bath, transitions between these levels occur due to angular momentum scattering. The system thus obeys a partially broken SU(3) symmetry. We show by exact numerical renormalization group (NRG) calculations that in a wide range of parameters the excited-state doublet $m = \pm 1$ is down-renormalized by Kondo correlation effects below the ground state of the non-interacting defect. Hence, this orbital momentum doublet becomes the Kondo degree of freedom, termed pseudospin $m = \pm 1$, and the quantum spin $\sigma = \pm 1/2$ of the fermionic bath particles constitutes the channel degree of freedom, conserved by the orbital angular momentum scattering. The degeneracy of the defect's orbital doublet is stabilized by spatial parity, while the channel degeneracy is guaranteed by time reversal symmetry. The NRG calculations unambiguously show that this model exhibits an extended 2CK phase. It may explain the 2CK signatures observed in the early point contact spectroscopy experiments by Ralph and Buhrman [13], including the conductance spikes at elevated bias and their splitting in a magnetic field, as proposed by us earlier [14, 15]. We also propose that this model may be realized physically in systems of ultracold atomic gases [16].

2. Model and numerical renormalization group

The system described above is represented by the model Hamiltonian [14, 15],

$$\mathcal{H} = \sum_{\mathbf{k}\sigma m} \varepsilon_{\mathbf{k}} c^\dagger_{\mathbf{k}\sigma m} c_{\mathbf{k}\sigma m} + \Delta_0 \sum_{m=\pm 1} f^\dagger_m f_m + \sum_\sigma \left[\frac{1}{2} J_z\, S_z\, s^\sigma_z + J_\perp \left(S_{1,-1} s^\sigma_{-1,1} + S_{-1,1} s^\sigma_{1,-1} \right) \right]$$
$$+ \sum_\sigma \sum_{\substack{m,n=-1,1 \\ n-m\in\pm 1}} \left[g^{(n)}_{m0}\, S_{m,0} s^\sigma_{n-m,n} + h.c. \right] + \sum_{m\pm 1} 2 g^{(0)}_{mm} S_{m,m} s^\sigma_{0,0}\,. \qquad (1)$$

Here the first term is the kinetic energy of the fermionic bath with spin $\sigma = \pm 1/2$; the second one describes the degenerate local doublet, $m = \pm 1$, with the level spacing Δ_0 above the impurity ground state, $m = 0$. The third, fourth and fifth terms describe the interactions between the impurity and the fermionic bath, where the capital operators $S_{m,n}$ denote the generators of SU(3) in the impurity Hilbert space and the lower-case operators $s_{m,n}$ denote the generators of SU(3) in the conduction electron Hilbert space, with coupling constants $J_z, J_\perp$, and $g^{(n)}_{m_f m_i}$ as defined in Fig. 1. The transitions within the unbroken SU(2) subgroup in the degenerate subspace of excited levels, $m = \pm 1$, are written explicitly as the third term. The dynamics of the impurity operators f_m, $f^\dagger_m$ are subject to the constraint that the impurity is in one of its three quantum states at any time, $\hat{Q} = \sum_{m=0,\pm 1} f^\dagger_m f_m = 1$. In Eq. (1), the angular momentum of the mobile fermions with respect to the impurity center, $m = 0, \pm 1$, is written explicitly, while the label $\mathbf{k}$ in the first term comprises all other, continuous fermion degrees of freedom. In order to keep the number of coupling constants simple, we will show only the results for $g^{(n)}_{m_f m_i} =: g$ and for Kondo coupling $J_\perp = J_z/2 =: J$ or for $J_\perp = J_z =: J$. All parameters are given in units of the unrenormalized half bandwidth D.

To analyze this model, we employed the NRG [17], adapting the algorithm outlined in Ref. [18] to the present case. Since the Hamiltonian has a large symmetry group of (partially broken) SU(3) $\times$ SU(2), the calculations are numerically demanding. Because the interaction involves

transitions between three levels [the fundamental representation of SU(3)], three Wilson chains are required. Each one comes in two flavors, the conserved SU(2) channel degree of freedom, spin $\sigma = \pm 1/2$. Therefore, each site of a Wilson chain has four states, $|0\rangle$, $|\uparrow\rangle$, $|\downarrow\rangle$, and $|\uparrow\downarrow\rangle$, i.e., in each renormalization group step the dimension of the Hilbert space grows by a factor $4^3 = 64$. We exploited symmetries of the model [19] so as to decompose the total Hilbert space into it's conserved subspaces and to gain efficiency of the computer code.

3. 2CK phase of the rotational defect model

In this section we present the results of our NRG analysis, in particular the phase diagram in the plane of Kondo coupling J and level spacing Δ_0 as well as the behavior of the Kondo temperature T_K and of the entropy $S(T)$ of the model in the 2CK phase. First we discuss how the 2CK fixed point is identified and distinguished from a trivial potential scattering fixed point in the renormalization group flow: For a Fermi liquid fixed point (single-channel Kondo or potential scattering) the fixed point spectrum alternates between even and odd number of NRG iterations, corresponding to even or odd total number of (pseudo)spins and due to the different energies of the (pseudo)spin singlet or (pseudo)spin doublet ($s = 1/2$) states, see Fig 2. For the 2CK fixed point there is no alternation of the spectra [19], because a complex spin-entangled state is formed, independent of the parity of the particle number in the system, see Fig 3. Furthermore, a Fermi liquid fixed point is characterized by an equidistant fixed point spectrum for large NRG iteration numbers, while the 2CK fixed point spectrum is not equidistant [19]. The qualitatively different fixed point spectra are shown in the NRG level flow diagrams of Figs. 2 (potential scattering) and 3 (2CK), respectively. While for the pure 2CK model [1] the fixed point level spacings are known from boundary conformal field theory [19], the fixed point spectrum of our extended model, Eq. (1), shows deviations from these values due to additional potential scattering terms present in our model. Nevertheless, the 2CK state may be distinguished from the Fermi liquid fixed point by the non-equidistant level spacing. Comparison of Figs. 2 and 3 shows that the system changes, for given values of J and g, from potential scattering to 2CK upon reducing the level spacing Δ_0.

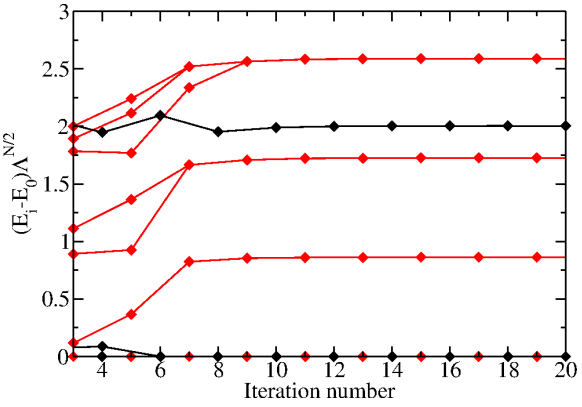

Figure 2. NRG energy level flow for the parameters $J = J_\perp = J_z/2 = 0.2$, $g = 0.002$, $\Delta_0 = 0.14$, and NRG discretization parameter $\Lambda = 4$ [18]. Potential scattering fixed point: alternation between even (black dots) and odd (red dots) number of iterations; equidistant fixed point spectra for even and odd iterations, respectively.

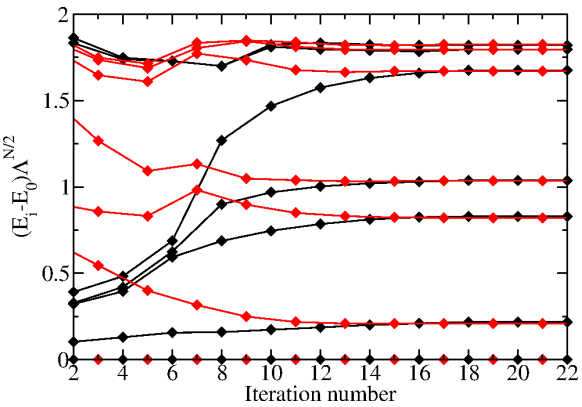

Figure 3. NRG energy level flow for the parameters $J = 0.2$, $g = 0.002$, $\Delta_0 = 0.13$, and NRG discretization parameter $\Lambda = 4$ [18]. 2CK fixed point: no alternation between even (black dots) and odd (red dots) number of iterations; non-equidistant fixed point spectrum.

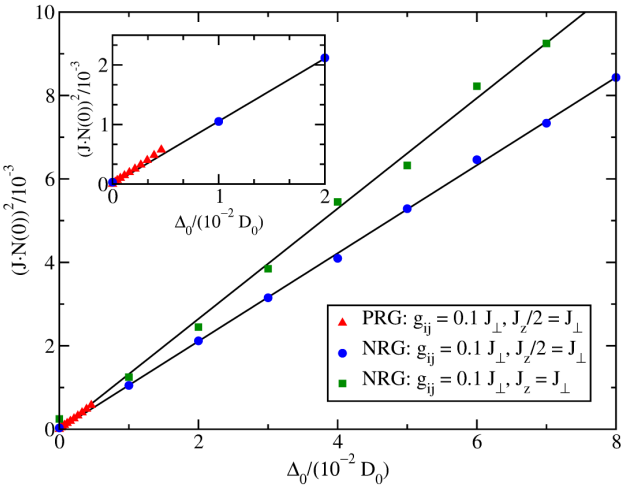

Figure 4. Phase diagram separating 2CK (above the line) and potential scattering (below the line) regimes for two different ratios of $J_z/J_\perp$, $J := J_\perp$, and $\Lambda = 3$ and iteration number $N = 25$. The green squares and blue circles are the results of NRG calculations. The red triangles are calculated with the PRG approach of Refs. [14, 15] for the parameter set of the blue data points.

Mapping out the different fixed points in the $N(0)J - \Delta_0$ plane, with N(0) the density of states at the Fermi energy, we obtain the phase diagram of our model as shown in Fig. 4. The data points shown are unstable fixed points separating the 2CK regime (above) from the trivial potential scattering regime (below the line). It is seen that the model generically exhibits an extended 2CK phase for a wide range of system parameters. In determining the phase boundary numerically, it must be observed that a minimal coupling strength $\bar{J}$ is necessary in order for the 2CK fixed point to be detectable by the NRG within N iteration steps. This threshold $\bar{J}$ must be subtracted from the numerically determined critical value of J in order to obtain the 2CK phase boundary that would be obtained after $N \to \infty$ iterations. $\bar{J}$ may be estimated as follows. The minimal resolvable energy by NRG after N steps is $E_{\min} = D \cdot \Lambda^{-N/2}$, where D is the half bandwidth and Λ the discretization parameter. The minimal Kondo temperature resolvable by NRG is, therefore, $T_{K\,\min} = D \exp[-1/(2N(0)\bar{J}] = E_{\min}$. Combining the last two equations, one obtains for the threshold, $N(0)\bar{J} = 1/N \ln \Lambda$, i.e., $N(0)\bar{J} = 0.0144$ for our NRG parameters N=25, $\Lambda = 3$. This threshold has been subtracted in the phase diagram, Fig. 4. Good quantitative agreement is found with the results of a perturbative renormalization group treatment for small coupling values, as described in Refs. [14, 15].

It is known that in the pure 2CK model [1] the 2CK fixed point corresponds to an intermediate coupling strength of $J^*/D \approx 0.7$ [19]. Hence, at this coupling strength T_K should reach up to the band width, $T_K^*/D \approx 1$, and decay exponentially on both sides of J^*. The latter has been shown due to a strong/weak coupling duality of the 2CK model [1, 20]. It is different from the single-channel Kondo model, where the fixed point is at strong coupling, $J \to \infty$. Our NRG calculations show that this behavior is also true for the rotational defect model, Eq. (1): Fig. 5 shows T_K for this model as a function of J for various values of the level spacing Δ_0, calculated by NRG. It exemplifies that large values of T_K may be realized in this model.

Finally, we discuss the temperature T dependence of the impurity contribution to the entropy $S(T)$, as shown in Fig. 6. For $T > \Delta_0$, all three impurity levels are thermally excited, and $S(T)/k_B = \ln 3$. As T is reduced below Δ_0, but $T > T_K$, the entropy obtains a plateau at $S(T)/k_B \approx \ln 2$. This indicates, that for $T < \Delta_0$ not the bare excited state doublet is frozen out, but a level crossing occurs induced by Kondo correlations, so that the $m = \pm 1$ doublet becomes the interacting impurity ground state and can host Kondo fluctuations even at the lowest energies. Because of the SU(2) channel symmetry, the system is then bound to flow to the 2CK fixed point for $T < T_K$. This is confirmed by the 2CK zero-point entropy of $S(0)/k_B = \ln \sqrt{2}$ [3] which is achieved in Fig. 6 at the plateau for $T \ll T_K$.

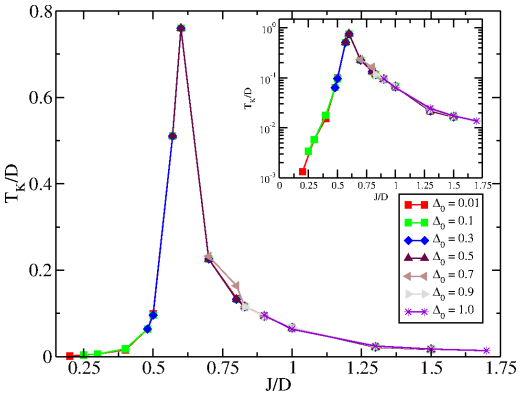

Figure 5. The Kondo temperature T_K as a function of the coupling constant $J = J_\perp = J_z/2$ is shown for various Δ_0 and for $g = 0.01J$. The inset shows the same on a logarithmic scale.

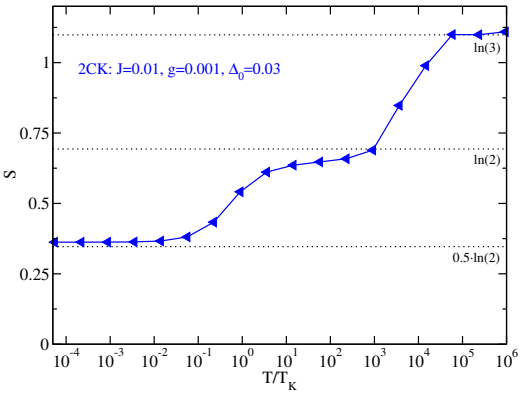

Figure 6. The impurity contribution to the entropy is shown as a function of temperature T. Three plateaus can be clearly distinguished, see text.

To summarize, we have demonstrated the existence of an extended 2CK phase in a rotational impurity model with partially broken SU(3) symmetry. We have also shown that at the 2CK fixed point coupling, $J^* \approx 0.7$, T_K reaches up to the band cutoff, as expected for a 2CK system, so that large T_K values can be achieved in this model.

Acknowledgments

We would like to thank Ralf Bulla, Alfred Zawadowski and Eran Sela for useful discussions. This work was supported in part by the DAAD (EFC), by the Alexander von Humboldt Foundation (LB) and by DFG through SFB 608.

References

[1] P. Nozières and A. Blandin, Journal de Physique (Paris), **41**, 193 (1980).
[2] A. M. Tsvelik and P. B. Wiegmann, Z. Phys. B **54**, 201 (1994).
[3] N. Andrei and C. Destri, Phys. Rev. Lett. **52**, 364 (1984);
[4] I. Affleck and A. W. W. Ludwig, Nucl. Phys. B, **352**, 849 (1991); Phys. Rev. Lett. **67**, 3160, (1991); Phys. Rev. B **48**, 7297 (1993).
[5] D. L. Cox and A. Zawadowski, Adv. Phys. **47**, 599 (1998).
[6] J. L. Black, K. Vladár, and A. Zawadowski, Phys. Rev. B **26**, 1559 (1982); K. Vladár and A. Zawadowski, Phys. Rev. B **28**, 1564 (1983); **28**, 1582 (1983); Phys. Rev. B **28**, 1596 (1983).
[7] I. L. Aleiner *et al.*, Phys. Rev. Lett. **86**, 2629 (2001).
[8] I. L. Aleiner and D. Controzzi, Phys. Rev. B **66**, 045107 (2002).
[9] C. L. Seaman *et al.*, Phys. Rev. Lett. **67**, 2882 (1991);
[10] T. Cichorek *et al.*, Phys. Rev. Lett. **94**, 236603 (2005).
[11] Y. Oreg, and D. Goldhaber-Gordon, Phys. Rev. Lett. **90**, 136602 (2003).
[12] R. M. Potok, I. G. Rau, H. Shtrikman, Y. Oreg, and D. Goldhaber-Gordon, Nature **446**, 167 (2007).
[13] D. C. Ralph and R. A. Buhrman, Phys. Rev. Lett. **69**, 2118 (1992); Phys. Rev. B **51** 3554 (1995).
[14] M. Arnold, T. Langenbruch, and J. Kroha, Phys. Rev. Lett. **99**, 186601 (2007).
[15] K. Ballmann and J. Kroha, Ann. Phys. (Berlin) **524**, No 3-4, 245-251 (2012).
[16] E. Fuh Chuo, K. Ballmann, L. Borda, and J. Kroha, in preparation.
[17] K. G. Wilson Rev. Mod. Phys. **47**, 775 (1975).
[18] R. Bulla, T. A. Costi, and Th. Pruschke, Rev. Mod. Phys. **80**, 395 (2008).
[19] H. B. Pang and D. L. Cox, Phys. Rev. B, **44**, 9454 (1991).
[20] Ch. Kolf and J. Kroha, Phys. Rev. B **75**, 045129 (2007).